American Mineralogist, Volume 94, pages 630–633, 2009

LETTER

Crystal structure and Raman spectrum of a high-pressure Li-rich majoritic garnet, $(Li_2Mg)Si_2(SiO_4)_3$

HEXIONG YANG,[1,*] JÜRGEN KONZETT,[2] ROBERT T. DOWNS,[1] AND DANIEL J. FROST[3]

[1]Department of Geosciences, University of Arizona, 1040 E. 4th Street, Tucson, Arizona 85721-0077, U.S.A.
[2]Institut für Mineralogie und Petrographie, Universität Innsbruck, Innrain 52, A-6020 Innsbruck, Austria
[3]Bayerisches Geoinstitut, Universität Bayreuth, Universitätsstrasse 30, D-95447 Bayreuth, Germany

ABSTRACT

A Li-rich majoritic garnet (LiMGt), $(Li_2Mg)Si_2(SiO_4)_3$, was synthesized at 15 GPa and 1500 °C and its structure studied with single-crystal X-ray diffraction and Raman spectroscopy. It is cubic with space group $Ia\bar{3}d$ and unit-cell parameters a = 11.2660(2) Å and V = 1429.91(1) Å^3. The 8-, 6-, and 4-coordinated cation sites in LiMGt are occupied by ($Li^+ + Mg^{2+}$), Si^{4+}, and Si^{4+}, respectively. Whereas the SiO_6 octahedron is nearly regular, the XO_8 dodecahedron is the most distorted of all known silicate garnets in terms of the bond-length distortion index. All Raman peaks of LiMGt are broader than those of pyrope, due to the substitution of Li^+ for Mg^{2+} at the dodecahedral site. Furthermore, both Si-O symmetric stretching (A_{1g}-ν_1) and O-Si-O symmetric bending (A_{1g}-ν_2) modes of LiMGt shift significantly to higher frequencies relative to the corresponding ones of pyrope. In contrast, the A_{1g}-(SiO_4) rotational mode of LiMGt displays a much lower frequency than that of pyrope. This study represents the first structural report on a garnet with an all-silicate framework and suggests that, like Na incorporation in garnets, the pressure-dependent coupled substitution of ($Li^+ + Si^{4+}$) for ($Mg^{2+} + Al^{3+}$) is likely one of the primary mechanisms for Li enrichment in garnets in the mantle and the transition zone.

Keywords: Majoritic garnet, crystal structure, Raman spectroscopy, high pressure

INTRODUCTION

Silicate garnets are one of the major rock-forming minerals in the Earth's crust and the upper mantle and may account for nearly 40–70% by volume of the transition zone between 410 and 660 km in depth (Agee 1998; Frost 2008). Most garnets from the Earth's crust possess cubic symmetry with space group $Ia\bar{3}d$ and the general chemical formula $X_3Y_2(SiO_4)_3$, where X = mainly Mg, Ca, Fe, or Mn, and Y = Al, Fe, or Cr. The garnet structure can be described as a three-dimensional network of alternating corner-shared SiO_4 tetrahedra and YO_6 octahedra, with larger X cations occupying interstitial 8-coordinated dodecahedral sites. Various cation substitutions may take place in garnets, giving rise to a wide range of technological and industrial applications, including solid-state lasers, oscillators, multipliers for electronics, low-dusting and highly productive abrasives for blast cleaning, waterjet cutting, sandpapers, effective and recyclable water filters, low-conductivity magnetic bobble domain devices, as well as popular colored gemstones.

At the upper mantle or transition zone pressures, garnets may become majoritic with considerable Si^{4+} in the Y site, such as $Mg_3(FeSi)(SiO_4)_3$ (Smith and Mason 1970), $Mn_3(MnSi)(SiO_4)_3$ (Fujino et al. 1986), $Mg_3(MgSi)(SiO_4)_3$ (Kato and Kumazawa 1985; Angel et al. 1989), $(Ca_{0.49}Mg_{2.51})(MgSi)Si_3O_{12}$ (Hazen et al. 1994a), and $Mg_3(Mg_xSi_xAl_{2-2x})(SiO_4)_3$ with $0.38 \leq x \leq 1.0$ (Nakatsuka et al. 1999). Intriguingly, a Na-rich majoritic garnet (NaMGt), $(Na_2Mg)Si_2(SiO_4)_3$, has been synthesized above 15 GPa and 1600 °C (Gasparik 1989; Pacalo et al. 1992; Bobrov et al. 2008). The discovery of NaMGt not only confirms the mechanism of Na incorporation into majoritic garnet through the pressure-dependent exchange reaction $Na^+ + Si^{4+} \leftrightarrow M^{2+} + Al^{3+}$ (Ringwood and Major 1971), but also suggests that Na concentrations may be used to estimate the formation pressure/depth of Na-bearing garnets. Recently, Bobrov et al. (2008) have determined phase relations in the $(Na_2Mg)Si_2(SiO_4)_3$-$Mg_3Al_2(SiO_4)_3$ system up to 24 GPa. However, no structure report has been available thus far for NaMGt. To contribute to the crystal-chemical knowledge of garnets containing significant amounts of monovalent cations, we present a structural study of a high-pressure synthetic Li-analog of NaMGt, namely $(Li_2Mg)Si_2(SiO_4)_3$, by means of single-crystal X-ray diffraction and Raman spectroscopy.

EXPERIMENTAL METHODS

The Li-rich majoritic garnet (LiMGt) sample used in this study was synthesized in a 1000t-multi anvil device. The starting material was prepared by mixing appropriate amounts of high-purity (≥99.99%) SiO_2, MgO, and Li_2CO_3 in an agate mortar under ethanol. The mixture was decarbonated by stepwise heating to 600 °C with intermittent checks of the loss on ignition. The oxide mix was then welded into a platinum capsule. The run conditions were 15 GPa and 1500 °C for 31.5 h. The detailed experimental procedures for the synthesis, electron microprobe analysis, and Raman spectrum measurement were similar to those described by Yang et al. (2009).

The composition of LiMGt was analyzed with a JEOL 8100 electron superprobe using 10 nA beam current and 15 kV acceleration voltage. Natural quartz and synthetic MgO were used as standards. Counting times on peaks and backgrounds

* E-mail: hyang@u.arizona.edu

of the X-ray lines were 20 and 10 s, respectively. Raw data were corrected using the PRZ procedure, which gave (wt%) SiO_2 = 82.0(2) and MgO = 11.8(1) (average of 11 analysis points). Li_2O was added to the EMP analyses to bring the total cation sums to 8.0 assuming a garnet stoichiometry based on 12 O atoms, yielding a chemical formula $(Li_{1.96}Mg_{1.04})(Si_{1.98}Mg_{0.02})(SiO_4)_3$.

Based on optical examination and X-ray diffraction peak profiles, a nearly equi-dimensional crystal was selected and mounted on a Bruker X8 APEX2 CCD X-ray diffractometer equipped with graphite-monochromatized Mo*K*α radiation. X-ray diffraction data were collected with frame widths of 0.5° in ω and 30 s counting time per frame. All reflections were indexed on the basis of a cubic unit-cell (Table 1). The intensity data were corrected for X-ray absorption using the Bruker program SADABS. The observed systematic absences of reflections indicated the unique space group $Ia\bar{3}d$.

The structure of LiMGt was solved and refined using SHELX97 (Sheldrick 2008). Anisotropic displacement parameters were refined for all atoms. During the refinements, the chemical composition was assumed to be stoichiometric $(Li_2Mg)Si_2(SiO_4)_3$. Final atomic coordinates and anisotropic displacement parameters are listed in Table 2[1] and selected bond distances and angles in Table 3.

Results and discussion

No dodecahedral site splitting is detectable in LiMGt. All anisotropic displacement amplitudes of the X (=Li + Mg) cation are similar to those of Mg in pyrope (Armbruster et al. 1992; Merli et al. 2000). Because of the similar radii of 8-coordinated Li^+ (r = 0.92 Å) and Mg^{2+} (r = 0.89 Å) (Shannon 1976), many geometrical parameters of the X site in LiMGt and pyrope are also comparable, e.g., mean X-O bond length, mean O-O edge distance, and dodecahedral volume (Table 3). Nonetheless, the dodecahedron in LiMGt is the most distorted of all silicate garnets, as measured by the bond-length distortion index (Renner and Lehmann 1986) or, more simply, by the difference between the two crystallographically independent X-O4 and X-O2 bond lengths [Δ(X-O)] (Ungaretti et al. 1995) (see Fig. 1 for the atom labels). The Δ(X-O) value for LiMGt is 0.1954 Å (Table 3), while it is only between 0.135 and 0.170 Å for 281 various silicate garnets examined by Ungaretti et al. (1995). The large distortion of the dodecahedral site in LiMGt can be understood on the basis of the tetrahedral rotation, α, about the $\bar{4}$ axis. This parameter is defined as $\tan\alpha = (y_{Si} - y_O)/(z_{Si} - z_O)$ (Born and Zemann 1964), where y_{Si}, z_{Si} , and y_O, z_O are the y and z coordinates of the Si and O atoms, respectively, when Si is placed at the origin. According to Meagher (1975), a decrease in α results in an increase in X-O4 more than in X-O2, and thus an increase in Δ(X-O). The α value for LiMGt is 23.28°, the smallest of all known silicate garnets (24.6–27.5°).

The SiO_6 octahedron in LiMGt is nearly regular in terms of the polyhedral angle variance (PAV) and quadratic elongation (PQE) (Robinson et al. 1971), with a mean Si-O bond distance of 1.777 Å, matching that (1.776 Å) in stishovite (Ross et al. 1990). The SiO_4 tetrahedron in LiMGt is less distorted than in pyrope (Table 3), as a consequence of the substitution of Li^+ for Mg^{2+} in the X site. Each SiO_4 tetrahedron shares two edges with the XO_8 dodecahedra, therefore the large tetrahedral distortion in pyrope originates chiefly from the need to reduce the strong repulsive

[1] Deposit item AM-09-022, Table 2, CIF, a data set, and Figure 2. Deposit items are available two ways: For a paper copy contact the Business Office of the Mineralogical Society of America (see inside front cover of recent issue) for price information. For an electronic copy visit the MSA web site at http://www.minsocam.org, go to the American Mineralogist Contents, find the table of contents for the specific volume/issue wanted, and then click on the deposit link there.

Table 1. Summary of crystal data and refinement results for high-pressure Li-majoritic garnet $(Li_2Mg)Si_2(SiO_4)_3$

Structural formula	$(Li_{1.96}Mg_{1.04})(Si_{1.98}Mg_{0.02})(SiO_4)_3$
Crystal size (mm)	0.08 x 0.08 x 0.06
Space group	*Iad* (No. 230)
a (Å)	11.2660(1)
V (Å^3)	1429.91(2)
Z	8
ρ_{calc} (g/cm^3)	3.44
λ (Å)	0.71069
μ (mm^{-1})	1.18
θ range for data collection	3.89 to 37.87
No. of reflections collected	13512
No. of independent reflections	331
No. of reflections with $I > 2\sigma(I)$	299
No. of parameters refined	19
R_{int}	0.036
Final *R* factors [$I > 2\sigma(I)$]	R_1= 0.022, wR_2=0.066
Final *R* factors (all data)	R_1= 0.025, wR_2=0.065
Goodness-of-fit	1.150

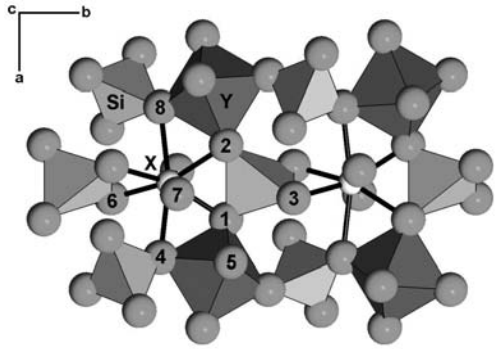

Figure 1. Crystal structure of Li-rich majoritic garnet viewed along the *c* axis.

Table 3. Selected interatomic distances (Å), O-M-O angles, and polyhedral distortions

	LiMGt	Pyrope
Si-O (x4)	1.6295(5)	1.6342(3)
O1-O2 (x2) (shared edge)	2.5020(5)	2.4968(3)
O1-Si-O2 (x2)	100.30(2)	99.61(1)
O1-O3 (x4) (unshared edge)	2.7371(5)	2.7507(3)
O1-Si-O3 (x4)	114.25(2)	114.62(1)
Mean O-O	2.6587	2.6660
PAV	51.92	59.98
PQE	1.013	1.015
α (rotation)	23.28	27.50
Y-O (x6)	1.7768(5)	1.8862(3)
O1-O4 (x6) (shared edge)	2.4978(5)	2.6165(3)
O4-O5 (x6) (unshared edge)	2.5277(5)	2.7161(3)
Mean O-O	2.5128	2.6663
PAV	0.51	5.04
PQE	1.000	1.001
X-O2 (x4)	2.1693(6)	2.1974(3)
X-O4 (x4)	2.3647(6)	2.3401(3)
Mean X-O	2.2670	2.2688
O1-O2 (x2) (shared with T)	2.5020(5)	2.4965(3)
O4-O7 (x2)	2.8172(5)	2.7781(3)
O1-O4 (x4) (shared with Y)	2.4978(5)	2.6165(3)
O4-O6 (x4)	2.8141(8)	2.7079(3)
Mean O-O	2.6572	2.6539

Notes: PAV = polyhedral angle variance in degrees squared; PQE = polyhedral quadratic elongation (Robinson et al. 1971).

interaction between Mg^{2+} and Si^{4+} (Mg^{2+}-Si^{4+} = 2.863 Å) across the shared O-O edges, making the two shared O-O edges of the SiO_4 tetrahedron shorter than the four unshared ones (Table 3). Any replacement of Mg^{2+} by Li^+ in the X site will be energetically favored because it will weaken the X-Si cation repulsion, thus reducing the tetrahedral distortion.

Examination of structural data for silicate garnets shows that the Si-O-Y angle (φ), which describes the linkage between the corner-shared SiO_4 tetrahedra and YO_6 octahedra, increases with increasing the r_X/r_Y ratio, where r_X and r_Y are the mean radii for the X and Y cations, respectively. For example, the φ angle is 130.7° in pyrope with r_X/r_Y = 1.664 (Armbruster et al. 1992), whereas it is 135.6° in grossular with r_X/r_Y = 2.094 (Geiger and Armbruster 1997). The φ and r_X/r_Y values for almandine, spessartine, uvarovite, and andradite all fall between those for pyrope and grossular. Although the r_X/r_Y ratio of LiMGt, 2.275, is the largest of all silicate garnets, its φ angle is only 135.12°, close to that of grossular. Thus, there appears to be an upper limit around 136° for the φ angle in silicate garnets, regardless of the relative X and Y cation sizes. Further support to this inference is that the φ angle in grossular is virtually unchanged at temperatures up to 675 °C (Meagher 1975).

Based on the measurement of relative compressibilities of silicate garnets, Hazen et al. (1994b) concluded that the behavior of the rigid tetrahedra-octahedra framework, rather than the dodecahedral sites, controls garnet compression, and that the compressibility of the framework is determined principally by the valence of the Y cations. Zhang et al. (1998) further pointed out that the φ angle in silicate garnets is probably restrained if the Y site is occupied by cations of high valence state, leading to a relatively stiff framework. The high bulk modulus (174–192 GPa) of NaMGt (Pacalo et al. 1992; Hazen et al. 1994b) appears to support this mechanism for garnet compression. Then, providing that silicate garnets obey Bridgman's law, which correlates bulk modulus inversely with ambient unit-cell volume for isostructural materials (Anderson and Anderson 1970; Hazen et al. 1994b), LiMGt, which has the smallest unit-cell volume of all known silicate garnets, should have a bulk modulus that is significantly greater than that for NaMGt.

Novak and Gibbs (1971) proposed empirical equations for estimating the unit-cell parameter, a, and O atomic coordinates (x_O, y_O, z_O) for a silicate garnet from r_X and r_Y. Using these equations and the effective ionic radii from Shannon (1976), we estimate a = 11.261 Å, x_O = 0.0316, y_O = 0.0449, z_O = 0.6484 for LiMGt. These values agree with our experimental data: a = 11.2660(3) Å, x_O = 0.03231(5), y_O = 0.04389(5), z_O = 0.64800(5). Surprisingly, the estimated a dimension of 11.533 Å for NaMGt is substantially greater than the value of 11.408(2) Å measured by Pacalo et al. (1992) or 11.410(1) Å by Hazen et al. (1994b). The reason for this is unclear. From the crystal-chemical point of view, the size difference between the eight-coordinated Na^+ (r = 1.18 Å) and Mg^{2+} (r = 0.89 Å) (Shannon 1976) is simply too large for them to form a complete solid solution. Perhaps, Na^+ and Mg^{2+} are ordered over crystallographically distinct sites in NaMGt, leading to a symmetry lower than that for garnet. Alternatively, the synthetic NaMGt may be a microscopic mixture of two phases. In fact, Gasparik (2000) has reported some experimental evidence for immiscibility in high Na-bearing garnets.

The Raman spectrum of LiMGt is compared to that of pyrope from the RRUFF project (http://rruff.info/R080060) in Figure 2[1]. Based on previous studies on pyrope and other silicate garnets (Hofmeister and Chopelas 1991; Chaplin et al. 1998; Kolesov and Geiger 1998, 2000; Hofmeister et al. 2004; Pascale et al. 2005), we made tentative assignments of observed Raman modes for LiMGt (Table 4) grouped into three distinct regions. The bands in the high- (800–1200 cm^{-1}) and middle-frequency (500–700 cm^{-1}) regions are attributed to internal modes of the SiO_4 unit, whereas the bands in the low-frequency (150–450 cm^{-1}) region include the rotational or translational modes of SiO_4 tetrahedra, as well as the X-cation motions. As expected, Raman peaks of LiMGt are all broader than those of pyrope, due to the local structural heterogeneities or atomic positional disorder caused by the size and charge differences between Mg^{2+} and Li^+ at the X site. Both Si-O symmetric stretching (A_{1g}-ν_1) and O-Si-O symmetric bending (A_{1g}-ν_2) modes of LiMGt shift significantly to higher frequencies relative to the corresponding ones of pyrope, indicating that the mean Si-O and O-O distances within the SiO_4 tetrahedra in LiMGt are shorter than those in pyrope, which is indeed the case (Table 3). Similar mode (A_{1g}-ν_1 and A_{1g}-ν_2) shifts to higher frequencies were also observed by Hofmeister et al. (2004) as pyrope becomes more majoritic. In contrast, the A_{1g}-R(SiO_4) mode of LiMGt displays a much lower frequency (316 cm^{-1}) than that (366 cm^{-1}) of pyrope. This observation can be explained by the weak constraint of the XO_8 dodecahedra imposed upon the SiO_4 tetrahedra in LiGMt. Because each SiO_4 tetrahedron shares two edges with XO_8 dodecahedra, when the X-O bond is weaker, as is the case of Li-O vs. Mg-O, the vibrational restoring force on the SiO_4 group is reduced. Hence, the SiO_4 group oscillates with a lower frequency.

Lithium contents in minerals from the mantle and ultrahigh-pressure metamorphic rocks have attracted considerable attention recently because they can provide important constraints on geochemical processes, such as partial melting, crystal fractionation, metasomatism, subduction, and low-temperature alteration (Seitz and Woodland 2000; Woodland et al. 2002; Paquin et al. 2004; Marschall et al. 2006). The following Li partition coefficients (D) have been determined for major rock-forming silicate minerals: $D^{olivine} > D^{clinopyroxene} \geq D^{orthopyroxene} >> D^{garnet}$ (Seitz and Woodland 2000; Woodland et al. 2002; Ottolini et al. 2004; Paquin et al. 2004; Marschall et al. 2006). However, from a systematic deter-

TABLE 4. Observed Raman modes and assignments for Li-majoritic garnet $(Li_2Mg)Si_2(SiO_4)_3$

Bands (cm^{-1})	Intensity	Assignment
	SiO_4 internal stretching modes	
1115	weak, broad	T_{2g}-ν_3 (Si-O) asymmetric stretching
989	medium, relatively broad	A_{1g}-ν_1 (Si-O) symmetric stretching
856	weak, broad	T_{2g}-ν_3 (Si-O) asymmetric stretching
	SiO_4 internal bending modes	
676	weak	T_{2g}-ν_4 (O-Si-O) asymmetric bending
599	very strong, sharp	A_{1g}-ν_2 (O-Si-O) symmetric bending
547	weak, shoulder	T_{2g}-ν_4 (O-Si-O) asymmetric bending
	Rotational/Translational modes	
347	weak, shoulder	T_{2g}-R(SiO_4) rotation
316	strong	A_{1g}-R(SiO_4) rotation
209	weak, broad	E_g or T_{2g}-T(SiO_4) or T(X) translation
157	very weak, broad	T_{2g}- T(X-O) translation

Note: X = (Li_2Mg).

mination of Li abundances in inclusions in diamonds of peridotitic, websteritic, eclogitic, and lower mantle paragenesis, Seitz et al. (2003) found that the Li partitioning among these minerals is a function of pressure and garnets containing a majorite component exhibit a dramatic increase in Li solubility, such that even for mildly majoritic garnets, $D^{\text{clinopyroxene}}/D^{\text{garnet}}$ can be smaller than one. This observation suggests that, similar to Na incorporation in garnets, the pressure-dependent coupled substitution of ($Li^+ + Si^{4+}$) for ($X^{2+} + Y^{3+}$) is likely one of the primary mechanisms for Li enrichment in garnets in the mantle and the transition zone. Nevertheless, as Na incorporation into garnets can also be achieved through other coupled substitutions, such as $Na^+ + Ti^{4+} \leftrightarrow M^{2+} + Al^{3+}$ (Haggerty et al. 1994), $Na^+ + P^{5+} \leftrightarrow M^{2+} + Si^{4+}$ (Thompson 1975; Haggerty et al. 1994; Brunet et al. 2006), or $Na^+ + M^{3+} \leftrightarrow 2\ M^{2+}$ (Enami et al. 1995), bulk compositional constraints may preclude its use as a geobarometer (Grütter and Quadling 1998). By analogy, Li concentrations in garnets may depend on bulk compositions as well. Thus, the general applicability of the Li-barometer to natural rocks representing a range in bulk compositions remains to be demonstrated.

ACKNOWLEDGMENTS

This study is supported by the Austrian Science Foundation (grant no. P17845-N10) and NSF (EAR-0609906).

REFERENCES CITED

Agee, C.B. (1998) Phase transformations and seismic structure in the upper mantle and transition zone. In R.J. Hemley, Ed., Ultrahigh-Pressure Mineralogy: Physics and Chemistry of the Earth's Deep Interior, 37, p. 165–203. Reviews in Mineralogy, Mineralogical Society of America, Chantilly, Virginia.

Anderson, D.L. and Anderson, O.L. (1970) The bulk modulus-volume relationship for oxides. Journal of Geophysical Research, 75, 3494–3500.

Angel, R.J., Finger, L.W., Hazen, R.M., Kanzaki, M., Weidner, D.J., Liebermann, R.C., and Veblen, D.R. (1989) Structure and twinning of single-crystal $MgSiO_3$ garnet synthesized at 17 GPa and 1800 °C. American Mineralogist, 74, 509–512.

Armbruster, T., Geiger, C.A., and Lager, G.A. (1992) Single-crystal X-ray structure study of synthetic pyrope almandine garnets at 100 and 293 K. American Mineralogist, 77, 512–521.

Bobrov, A.V., Kojitani, H., Akaogi, M., and Litvin, Y.A. (2008) Phase relations on the diopside-jadeite-hedenbergite join up to 24 GPa and stability of Na-bearing majoritic garnet. Geochemica et Cosmochimica Acta, 72, 2392–2408.

Born, L. and Zemann, J. (1964) Abstandsberechnung und gitterenergetische Berechnungen an Granaten. Contributions to Mineralogy and Petrology, 10, 2–23.

Brunet, F., Bonneau, V., and Irifune, T. (2006) Complete solid solution between $Na_3Al_2(PO_4)_3$ and $Mg_3Al_2(SiO_4)_3$ garnets at high pressure. American Mineralogist, 91, 211–215.

Chaplin, T., Price, G.D., and Ross, N.L. (1998) Computer simulation of the infrared and Raman activity of pyrope garnet, and assignment of calculated modes to specific atomic motions. American Mineralogist, 83, 841–847.

Enami, M., Cong, B., Yoshida, T., and Kawabe, I. (1995) A mechanism for Na incorporation in garnet: An example from garnet in orthogneiss from the Su-Lu terrane, eastern China. American Mineralogist, 80, 475–482.

Frost, D.J. (2008) The upper mantle and transition zone. Elements, 4, 171–176.

Fujino, K., Momoi, H., Sawamoto, H., and Kumazawa, M. (1986) Crystal structure and chemistry of $MnSiO_3$ tetragonal garnet. American Mineralogist, 71, 781–785.

Gasparik, T. (1989) Transformation of enstatite-diopside-jadeite pyroxenes to garnet. Contributions to Mineralogy and Petrology, 102, 389–405.

——— (2000) Evidence for immiscibility in majorite garnet from experiments at 13–15 GPa. Geochimica et Cosmochimica Acta, 64, 1641–1650.

Geiger, C.A. and Armbruster, T. (1997) $Mn_3Al_2Si_3O_{12}$ spessartine and $Ca_3Al_2Si_3O_{12}$ grossular garnet: Structural dynamics and thermodynamic properties. American Mineralogist, 82, 740–747.

Grütter, H.S. and Quadling, K.E. (1998) Can sodium in garnet be used to monitor eclogitic diamond potential? In J.J. Gurney, J.L. Gurney, M.D. Pascoe, and S.H. Richardson, Eds., Proceedings of the VIIth International Kimberlite Conference, p. 314–320. National Book Printers, Goodwood, South Africa.

Haggerty, S.E., Fung, A.T., and Burt, D.M. (1994) Apatite, phosphorus and titanium in eclogitic garnet from the upper mantle. Geophysical Research Letters, 21, 1699–1702.

Hazen, R.M., Downs, R.T., Finger, L.W., Conrad, P.G., and Gasparik, T. (1994a) Crystal chemistry of Ca-bearing majorite. American Mineralogist, 79, 581–584.

Hazen, R.M., Downs, R.T., Conrad, P.G., Finger, L.W., and Gasparik, T. (1994b) Comparative compressibilities of majorite-type garnets. Physics and Chemistry of Minerals, 21, 344–349.

Hofmeister, A.M. and Chopelas, A. (1991) Vibrational spectroscopy of end-member silicate garnets. Physics and Chemistry of Minerals, 17, 503–526.

Hofmeister, A., Giesting, P., Wopenka, B., Gwanmesia, G., and Jolliff, B. (2004) Vibrational spectroscopy of pyrope-majorite garnets: Structural implications. American Mineralogist, 89, 132–146.

Kato, T. and Kumazawa, M. (1985) Garnet phase of $MgSiO_3$ filling the pyroxeneilmenite gap at very high temperature. Nature, 316, 803–805.

Kolesov, B.A. and Geiger, C.A. (1998) Raman spectra of silicate garnets. Physics and Chemistry of Minerals, 25, 142–151.

——— (2000) Low-temperature single-crystal Raman spectrum of pyrope. Physics and Chemistry of Minerals, 27, 645–649.

Marschall, H.R., Alther, R., Ludwig, T., Kalt, A., Gmeling, K., and Kasztovszky, Z. (2006) Partitioning and budget of Li, Be, and B in high-pressure metamorphic rocks. Geochimica et Cosmochimica Acta, 70, 4750–4769.

Meagher, E.P. (1975) The crystal structures of pyrope and grossularite at elevated temperatures. American Mineralogist, 60, 218–228.

Merli, M., Ungaretti, L., and Oberti, R. (2000) Leverage analysis and structure refinement of minerals. American Mineralogist, 85, 532–542.

Nakatsuka, A., Yoshiasa, A., Yamanaka, T., Ohtaka, O., Katsura, T., and Ito, E. (1999) Symmetry change of majorite solid-solution in the system $Mg_3Al_2Si_3O_{12}$-$MgSiO_3$. American Mineralogist, 84, 1135–1143.

Novak, G.A. and Gibbs, G.V. (1971) The crystal chemistry of the silicate garnets. American Mineralogist, 56, 791–825.

Ottolini, L., Le Fèvrea, B., and Vannucci, R. (2004) Direct assessment of mantle boron and lithium contents and distribution by SIMS analyses of peridotite minerals. Earth and Planetary Science Letters, 228, 19–36.

Pacalo, R.E.G., Weidner, D.J., and Gasparik, T. (1992) Elastic properties of sodium-rich majorite garnet. Geophysical Research Letters, 19, 1895–1898.

Paquin, J., Altherr, R., and Ludwig, T. (2004) Li–Be–B systematics in the ultrahigh-pressure garnet peridotite from Alpe Arami (Central Swiss Alps): Implications for slab-to-mantle transfer. Earth and Planetary Science Letters, 218, 507–519.

Pascale, F., Zicovich-Wilson, C.M., Orlando, R., Roetti, C., Ugliengo, P., and Dovesi, R. (2005) Vibration frequencies of $Mg_3Al_2Si_3O_{12}$ pyrope. An ab initio study with the CRYSTAL code. Journal of Physical Chemistry, B109, 6146–6152.

Renner, B. and Lehmann, G. (1986) Correlation of angular and bond length distortions in TO_4 units in crystals. Zeitschrift für Kristallographie, 175, 43–59.

Ringwood, A.E. and Major, A. (1971) Synthesis of majorite and other high-pressure garnets and perovskites. Earth and Planetary Science Letters, 12, 411–418.

Robinson, K., Gibbs, G.V., and Ribbe, P.H. (1971) Quadratic elongation, a quantitative measure of distortion in coordination polyhedra. Science, 172, 567–570.

Ross, N.L., Shu, J., Hazen, R.M., and Gasparik, T. (1990) High pressure crystal chemistry of stishovite. American Mineralogist, 75, 739–747.

Seitz, H.-M. and Woodland, A.B. (2000) The distribution of lithium in peridotitic and pyroxenitic mantle lithologies—An indicator of magmatic and metamorphic processes. Chemical Geology, 47–64.

Seitz, H.-M., Brey, G.P., Stachel, T., and Harris, J.W. (2003) Li abundances in inclusions in diamonds from upper and lower mantle. Chemical Geology, 201, 307–318.

Shannon, R.D. (1976) Revised effective ionic radii and systematic studies of interatomic distances in halides and chalcogenides. Acta Crystallographica, A32, 751–767.

Sheldrick, G.M. (2008) A short history of SHELX. Acta Crystallographica, A64, 112–122.

Smith, J.V. and Mason, B. (1970) Pyroxene-garnet transformation in Coorara meteorite. Science, 168, 832–833.

Thompson, R.N. (1975) Is upper mantle phosphorus contained in sodic garnet? Earth and Planetary Science Letters, 26, 417–424.

Ungaretti, L., Leona, M., Merli, M., and Oberti, R. (1995) Non-ideal solid-solution in garnet: crystal-structure evidence and modeling. European Journal of Mineralogy, 7, 1299–1312.

Woodland, A.B., Seitz, H.-M., Alther, R., Marschall, H., Olker, B., and Ludwig, T. (2002) Li abundance in eclogite minerals: a clue to a crustal or mantle origin? Contributions to Mineralogy and Petrology, 143, 587–601.

Yang, H., Konzett, J., Frost, D.J., and Downs, R.T. (2009) X-ray diffraction and Raman spectroscopic study of clinopyroxenes with six-coordinated Si in the $Na(Mg_{0.5}Si_{0.5})Si_2O_6$-$NaAlSi_2O_6$ system. American Mineralogist, in review.

Zhang, L., Ahsbahs, H., and Kutoglu, A. (1998) Hydrostatic compression and crystal structure of pyrope to 33 GPa. Physics and Chemistry of Minerals, 25, 301–307.

MANUSCRIPT RECEIVED NOVEMBER 11, 2008
MANUSCRIPT ACCEPTED DECEMBER 4, 2008
MANUSCRIPT HANDLED BY BRYAN CHAKOUMAKOS